ScienSage

Journal of Advanced Scientific Research

Available online through http://www.sciensage.info

ISSN
0976-9595
Research Article

MICROWAVE-ASSISTED GREEN SYNTHESIS OF SILVER NANOPARTICLES USING PASSION FRUIT PEEL EXTRACT FOR CATALYTIC REDUCTION OF ORGANIC DYES

Vani Vangari, Yaku Gugulothu, Areef Mohammed, Umesh Kumar U*, Panasa Reddy A

Department of Chemistry, Osmania University, Hyderabad, Telangana state, India

**Corresponding author: utkoor@gmail.com*

ABSTRACT

Microwave-assisted synthesis of silver nanoparticles (AgNPs) was investigated using passion fruit peel (PF) extract as a stabilizer and reductant. In synthesis process, the effect of several synthetic factors such as pH, silver nitrate concentration and microwave irradiation time were studied. The obtained AgNPs were well characterized by several analytical techniques including UV-vis, FTIR, XRD, TEM and zeta-potential. The presence of strong surface plasmon resonance (SPR) peak around 400-410 nm indicated the formation of AgNPs. FTIR analysis revealed the biomolecules present in the PF extract was responsible for the reduction of silver ions and stabilization of formed AgNPs. The TEM images presented that the formed AgNPs were dispersed, nearly spherical shape and with average diameter of 12±3 nm. The powder XRD patterns of AgNPs revealed the face-centered cubic (FCC) structure. The catalytic activity of AgNPs was evaluated by $NaBH_4$ mediated reduction of Methylene Blue (MB) and Rhodamine B (RhB) and the kinetic analysis revealed pseudo-first-order nature of these reactions.

Keywords: Green synthesis, Microwave, Passion fruit peel, Dye removal.

1. INTRODUCTION

Water pollution caused by the chemicals released from dye industries, is a major concern. These dye pollutants are toxic and produce strong color even at very low concentrations [1]. Hence, removal of dye pollutants is a highly needed. Currently, several techniques such as adsorption, photocatalysis are in use to treat the dye polluted water. However, these conventional techniques require high energy and time consuming [2]. Hence, finding a rapid and efficient technique is the quest. Recently, noble metal nanoparticles based catalysis is widely explored for this application. Among all metal nanoparticles (MNPs), AgNPs received great attention with low cost, high catalytic activity and easy synthesis [3].

Nanoparticles possess interesting properties compared to their bulk counter parts. Recently MNPs have gained tremendous attention with their fascinating optical, electronic and catalytic properties [4]. They found wide applications in the fields ranging from catalysis, optical, optoelectronics, and biomedicine. Among various MNPs, AgNPs received great attention with their low cost, strong antimicrobial properties, catalytic and optical properties [5].

Conventional methods of AgNPs preparation generally involve the usage of toxic chemicals, organic solvents, and require high energy [6]. With the growing concern on environmental protection, recently green synthesis methods were developed [7]. Green methods generally involve the usage of water solvent, nontoxic bio-based materials as reducing and stabilizing agents and low energy. Recently, several researchers reported the preparation of AgNPs using plant based materials [8]. The fruit of *Passiflora edulis*, commonly known as passion fruit is widely used in food industry due to its high vitamin C content. The fruit peel accounts almost half of the fruit weight and is considered as waste. Phytochemical analysis studies revealed that the passion fruit peel contains various polyphenolic compounds such as carotenoids and flavonoids [9]. These compounds are well known for their antioxidant capacity and can serve as reducing and capping agent for MNPs preparation[10].

Microwave irradiation (MWI) has recently received a lot of interest as a promising new technique for the one-pot synthesis of MNPs in solutions. MWI is known to create localized superheating, which keeps nanoparticles nucleating and growing uniformly [11]. Compared to

conventional heating, microwave irradiation is considered as green method and it drastically reduces the reaction time [12].

In the current study, we have described the biogenic synthesis of AgNPs using an aqueous extract of passion fruit peel (PF) wherein the synthesis was performed employing microwave irradiation approach. AgNPs were characterized using various techniques to measure the absorption properties, particle morphology, size, crystal structure and Zeta potential etc. Moreover, the as-prepared AgNPs is employed as eco-friendly catalyst for reduction of MB and RhB in the presence of $NaBH_4$ and their reaction kinetics is also reported.

2. EXPERIMENTAL

2.1. Material

Fresh fruit of *Passiflora edulis* was collected from local market in Hyderabad, Telangana, India. Silver nitrate ($AgNO_3$), $NaBH_4$, Methylene blue (MB) and Rhodamine B (RhB) were purchased from S.D. Fine Chemicals, Mumbai, India. All of the chemicals employed in this investigation were of analytical quality and were used without additional treatment, and the experiment was carried out entirely using double distilled water (DDW).

2.2. Preparation of extract

Fresh fruit of *Passiflora edulis* was cut and the peel was collected. The peel was cut into small pieces, washed and dried in shade. Finally, they were oven dried for 1 hour at 80°C and blend to make a fine powder. The PF extract was prepared by boiling 1 g of powder in 100 mL DDW. Finally, allowed to cool and filtered using Whatman filter paper.

2.3. Synthesis of silver nanoparticles

At first, the above prepared 1% extract was diluted to 0.25% and 10 mM $AgNO_3$ stock solution was prepared. For AgNPs synthesis, 3 mL of extract is added with different volumes of 10 mM $AgNO_3$. The pH of the mixed solution was adjusted to 11 by adding 1M NaOH. Finally, the reaction mixture was taken in a sealed glass vial and subjected to microwave irradiation for 30s. A domestic microwave oven operating at 700 W was employed. After allowing to cool down naturally, the solution was centrifuged at 10000 RPM for 15 min and the pellet was retrieved. Then, the pellet was dispersed in a 10 mL DDW for further study.

2.4. Characterization techniques

Various analytical methods were used to characterize the produced nanoparticles. Using Cu-Kα radiation (= 0.15406 nm), powder X-ray diffraction (XRD, RigakuMiniflex 600) was utilized to identify the crystal structure and phase purity of the as-prepared nanoparticles. The optical absorbance was measured using a UV-visible spectrophotometer (Shimadzu, UV-2600) at wavelengths ranging from 200 to 800 nm. Shimadzu IR Prestige-21 spectrophotometer was used to identify the phytochemicals involved in metal reduction and stabilization of the produced nanoparticles. The materials were ground with KBr to create a pellet, and the FTIR spectra were collected in the 4000 to 400 cm^{-1} region.The size and shape of the as-prepared nanoparticles were determined using a Transmission Electron Microscope (TEM, JEOL JEM 2100) set at 200 kV. The crystalline structure of produced AgNPs was investigated using a selected area electron diffractogram. The zeta potential was used to determine the stability of NPs (DLS, Malvern instrument Ltd., Malvern, UK).

2.5. Catalytic activity

In a typical experiment, a 2 mL of MB or RhB solution (10 mg/L) was taken in a quartz cuvette, then 1 mL of 10mM $NaBH_4$ solution and AgNPs (100 µL) were added. The reduction reaction was then monitored by recording the UV-visible absorption spectra. Control experiments were also performed in the absence of AgNPs. Kinetics of the reduction reaction was obtained by noticing UV-vis absorbance at 663 nm for MB and 553 nm for RhB, respectively.

3. RESULTS AND DISCUSSION

The present work involves the microwave-assisted preparation of AgNPs using PF extract as reducing and capping agent and exploration of their catalytic activity (scheme 1). To optimize AgNPs synthesis, the effect of pH, $AgNO_3$ concentrations and microwave time were studied.

3.1. Synthesis

The UV-visible spectroscopy has been used for the preliminary conformation of AgNPs formation. In general, the spectrum shows the SPR band centered around 400-440 nm which is a characteristic peak of AgNPs [13]. In this work, we used SPR as a probe to optimize the reaction conditions and its growth kinetics.

Fig.1 shows the UV-visible absorption spectrum of as-prepared AgNPs at pH conditions. The initial pH of the reaction mixture was found 5.1 and at this pH, the synthesis of AgNPs was unsuccessful. According to previous reports, alkaline pH encourages the AgNPs formation [14]. Hence, we have adjusted to the pH with NaOH and studied the AgNPs formation. Interestingly, the addition of NaOH to the extract (in the absence of $AgNO_3$) also produced yellow coloration. This might be due to the deprotonation of polyphenol present in the extract. The yellow coloration of the extract can be confused with the yellow color of the AgNPs formation. Hence, to avoid such confusion, at each pH, we have recorded the absorption spectra of the extract and prepared AgNPs. As shown in Fig.1, with increase in the pH the solution turned yellow color and exhibited absorption peak at around 380 nm. After microwave irradiation, the formation of AgNPs were observed. At pH 7.4, the formation was little, with increase in the pH, AgNPs formation was also increased. The samples at pH 9, 10.2, 11, and 12 were diluted 5 times to record a clear spectrum.

Scheme 1: Flowchart of preparation of PF capped AgNPs and its application for catalytic activity.

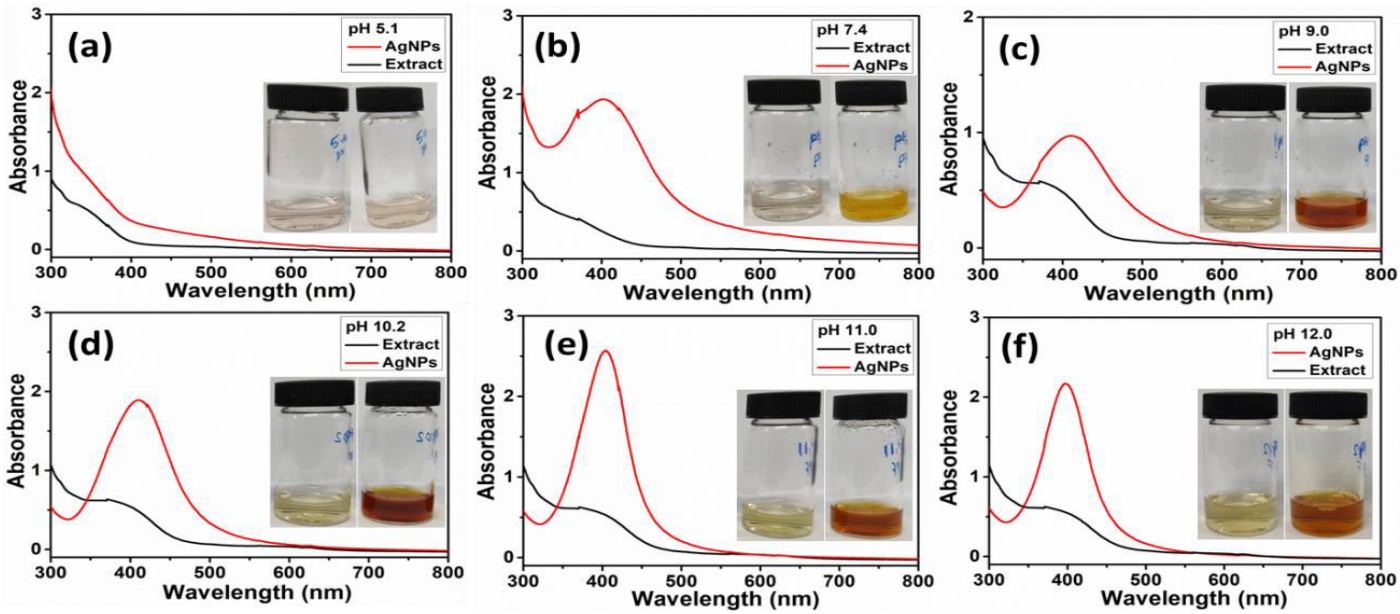

In each spectrum, black line showing the absorption at the particular pH and red line showing the absorption of AgNPs after microwave irradiation

Fig. 1: Effect of solution pH on AgNPs formation

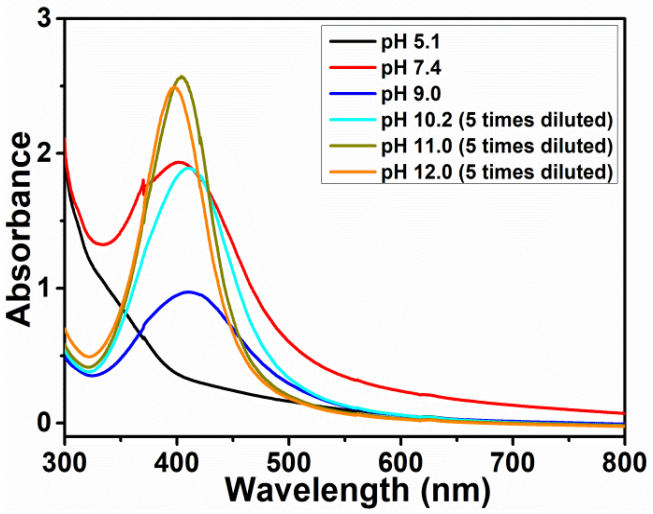

Fig. 2: Comparative absorbance spectra of AgNPs prepared at different pH values.

Comparative spectra of AgNPs prepared at different pH values is displayed in Fig. 2. As shown in figure, at low pH values (7 and 9) a broad absorption peaks were observed. This indicates the formation of AgNPs with different sizes. With increase in the pH, the peaks became narrow indicating the formation of uniform particles. Furthermore the peaks shifted to low wavelength side indicating the decrease in the particle size. pH 11 was found optimal and further increase in the pH caused a decrease in the absorbance.

Effect of $AgNO_3$ concentration and microwave irradiation time was further investigated. As shown in Fig 3a, with increase in the $AgNO_3$ concentration from 0.25 to 1.25 mM, the absorption peak clearly increased. This indicates the formation of AgNPs is also increased. However, further increase in the $AgNO_3$ concentration resulted in only a slight increase in the absorbance. Hence, 1.25 mM $AgNO_3$ was selected as optimum. Effect of microwave irradiation on AgNPs formation is shown in Fig 3b. Interestingly, 10 s of microwave irradiation was also sufficient to produce AgNPs. With further increase in the time, formation was also increased. 25 s of microwave irradiation was found sufficient for maximum AgNPs formation. Further increase in the irradiation time to 30 s resulted in a slight decrease in the absorbance.

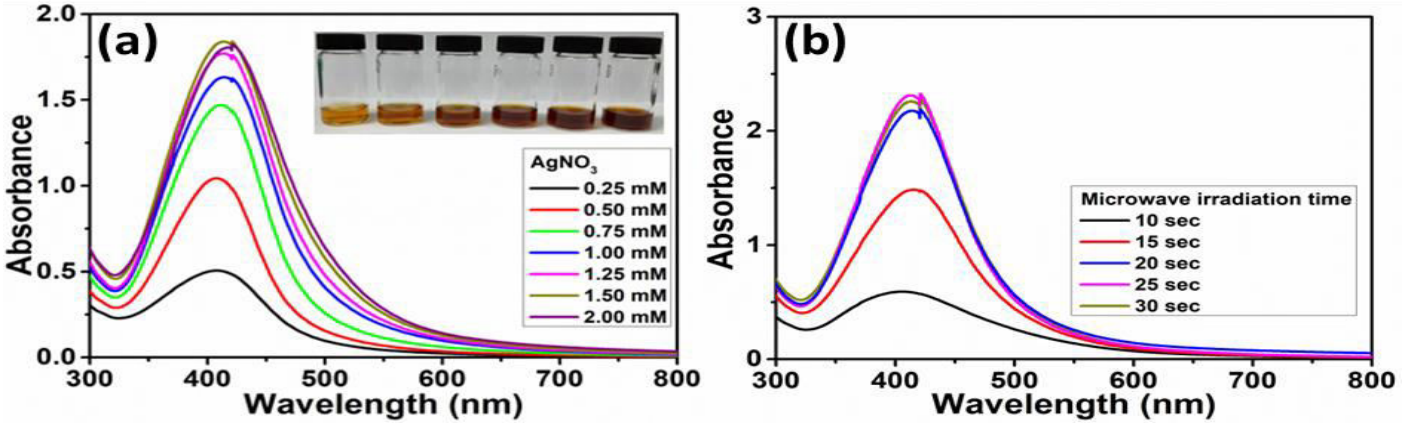

Fig. 3: (a) Effect of $AgNO_3$ concentration and (b) effect of microwave irradiation time on AgNPs formation

3.2. Characterization

3.2.1. Transmission electron microscopy (TEM)

As shown in Fig. 4 (a), the particles formed were nearly spherical in shape, highly dispersed with few aggregated particles. Corresponding particle size distribution histogram is shown in Fig.4b. AgNPs were in the size range of 6-23 nm and the average size was found to be 12±3 nm. Moreover, the HRTEM image Fig. 4 (c) shows that the lattice fringe spacing is 0.24nm, implying that the growth of the AgNPs is mostly in the (111) plane [15]. In addition, the information obtained from SAED pattern (Fig. 4d) revealed concentric rings with bright spots assigning a highly crystalline structure of AgNPs. These rings can be attributed to the diffraction from the (111), (200), (220) and (311) planes of FCC of metallic silver and it is clear that (111) lattice plane is the favored orientation for the generated AgNPs [16].

3.2.2. X-ray diffraction (XRD) analysis

Powder XRD patterns of the PF and PF stabilized AgNPs were shown in Fig 5. As shown in figure, pure PF shows the amorphous nature whereas AgNPs have

shown four distinct characteristic diffraction peaks at 38. 23° (111), 44.34° (200), 64. 48° (220) and 77.54° (311) which are attributed to the FCC crystal structure of metallic silver (JCPDS file no. 04-0783), similar peaks were observed in previous report [17]. Among all diffraction peaks, the highest reflection was detected at (111) planes, indicating the most preferable growth direction of AgNPs. The average crystal size was calculated using Scherrer equation. $D = 0.9\lambda/\beta \cos\theta$, where D is average crystal size, λ is wavelength of radiation (0.154 Å), β is full width at half maximum and θ is diffraction angle. The obtained average crystallite size is 10.12 nm, which is in accordance with TEM result.

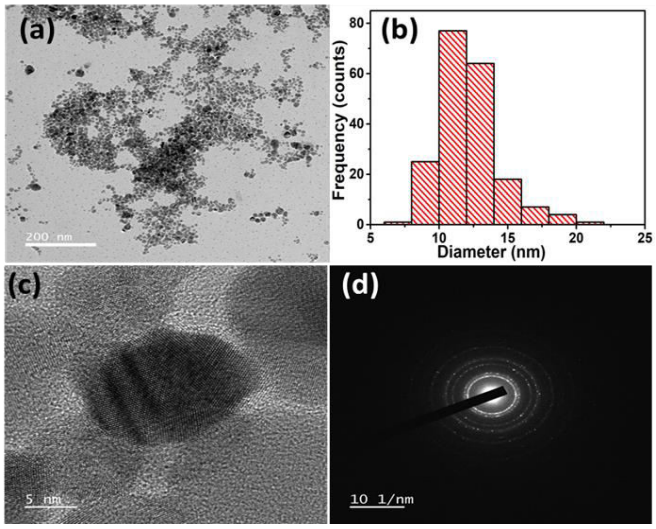

Fig. 4: (a) TEM image of AgNPs, (b) corresponding particle size distribution histogram (c) HRTEM image of one particle, and (d) SAED pattern

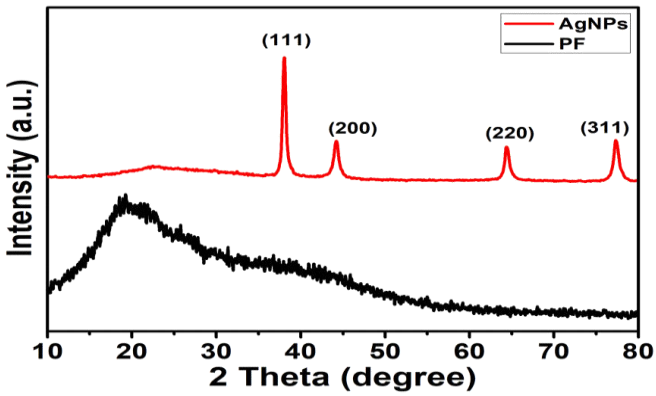

Fig. 5: X-ray diffraction patterns of PF and PF stabilized AgNPs

3.2.3. Zeta potential analysis

The charge on NPs was determined using the zeta potential. The zeta potential of AgNPs is seen in Fig. 6. This indicates the existence of repulsive forces and can be used to predict nanoparticle stability [18]. As a dispersant, AgNPs have a negative zeta potential of -36.3 mV. Due to this negative potential, the formed AgNPs can be attributed to their high stability and no agglomeration up to two month.

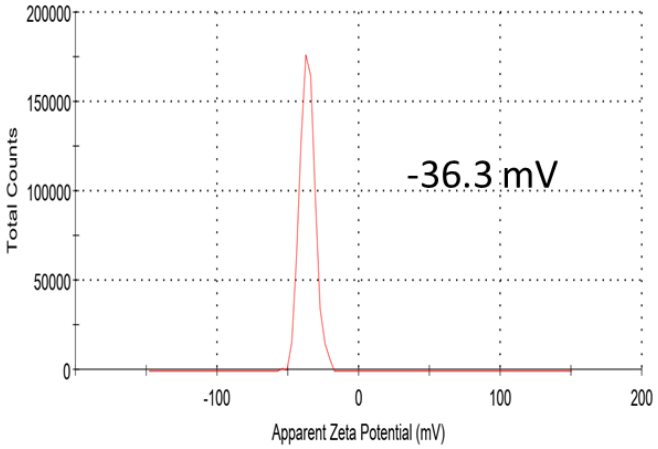

Fig. 6: Zeta potential of PF stabilized AgNPs

3.2.4. Fourier Transform Infrared spectroscopy (FTIR)

The FTIR spectra of PF and PF capped AgNPs are shown in Fig.7. The broad band observed at 3442 cm^{-1} corresponds to the stretching vibration of O-H groups in PF [10].

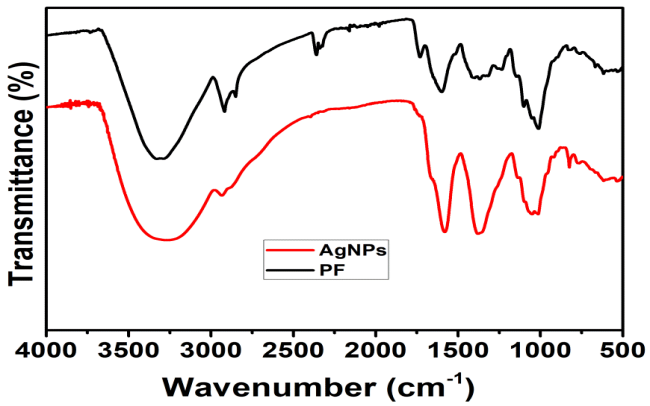

Fig. 7: FTIR spectra of PF and PF stabilized AgNPs

The band at 2870 cm^{-1} can be assigned to symmetric stretching vibrations of aliphatic -CH_3 groups present in

the PF. The peaks at 1645 and 1380 cm^{-1}can be ascribed to the characteristic asymmetrical and symmetrical stretching vibrations of the -COO^-group. The peak at 1068 cm^{-1}can be accredited to stretching vibrations of the C-O bond in ether group [19]. A clear shifts in peak positions were observed in FTIR spectra of both the PF extract and PF stabilized AgNPs that the shifting of peaks from 3470 to 3442 cm^{-1}, 2876 to 2870 cm^{-1}, 1662 to 1645 cm^{-1}, and 1073 to 1068 cm^{-1} with decreased peak intensity suggesting that hydroxyl, methyl, carboxylate, and carbonyl functional groups are involved in the formation and stability of AgNPs.

3.3. Catalytic activity

Figs. 8 and 9 depict the catalytic reduction reactions of MB and RhB, respectively. The absorption spectra of MB and RhB, as shown in Figs. 8a and 9a, were centered at 663 nm and 553 nm, respectively [20]. There was no significant variation in absorption peak intensities when only $NaBH_4$ was added. However, with the addition of AgNPs, the peaks steadily dropped with time, and the reduction was accomplished in 12 minutes (Fig 8b and 9b).The concentration of $NaBH_4$ in these reduction reactions was greater than that of the reduced products and remained constant throughout the process. As a result, the pseudo-first order reaction kinetics may be used to assess the catalytic activity of AgNPs; this sort of kinetics has been seen in recent results. Figs. 8c and 9c show a plot of ln (A_0/A_t) against time for the catalytic reduction of these dyes using AgNPs, where A_t and A_0 represent absorption intensities at time t and 0, respectively. The estimated rate constant for MB is 0.296 min^{-1}, while the rate constant for RhB is 0.335 min^{-1}.A controlled experiment conducted without the addition of a catalyst revealed no significant changes in absorption intensities even after 60 minutes, confirming the catalytic activity of as-prepared AgNPs.

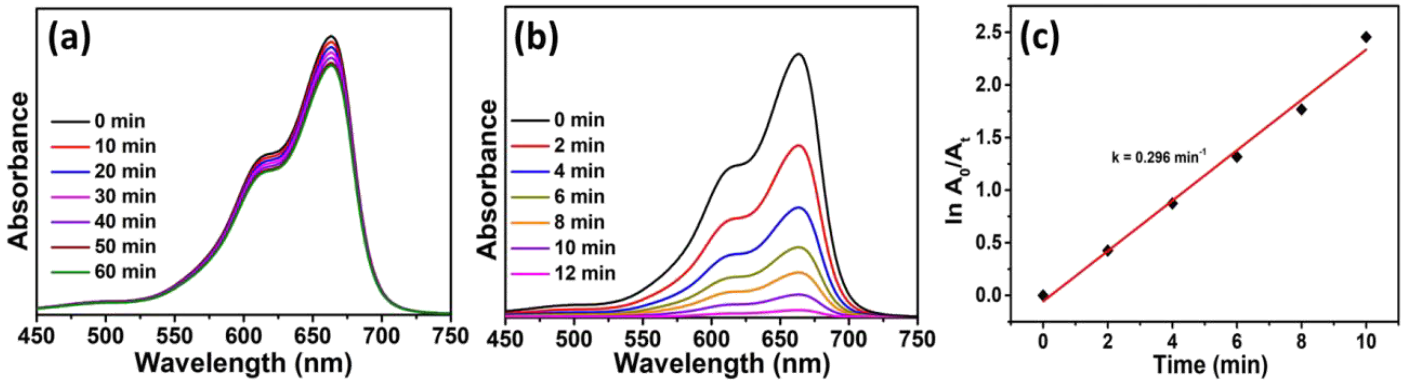

(a) in the presence of $NaBH_4$ and in the absence of AgNPs (b) in the presence of $NaBH_4$ and AgNPs, (c) the pseudo-first order kinetics of reduction reaction

Fig. 8: UV-visible absorption spectra of MB reduction

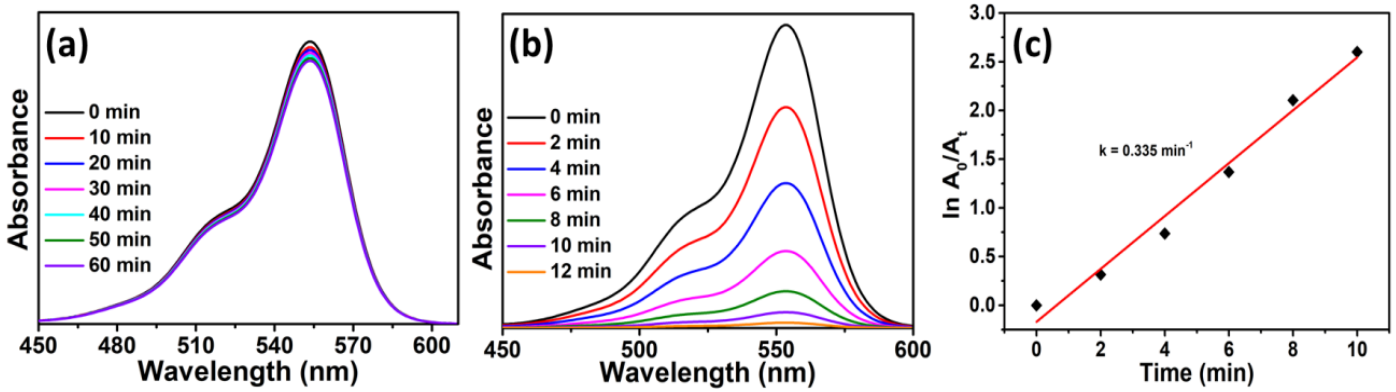

(a) *in the presence of $NaBH_4$ and in the absence of AgNPs (b) in the presence of NaBH4 a$_n$d AgNPs, (c) the pseudo-first order kinetics of reduction reaction*

Fig. 9: UV-visible absorption spectra of RhB reduction

4. CONCLUSION

In conclusion, the microwave method was effectively used to create AgNPs utilizing Passion fruit peel extract as a reducing and stabilizing agent, and the process of production was addressed. Importantly, the absorption spectra of nanoparticles were carefully adjusted by optimizing various process parameters for their production, including extract pH, $AgNO_3$ concentration, and microwave duration. FTIR analyses were used to identify the phytochemicals contained in the extract. The TEM images revealed that the generated AgNPs were around 12±3 nm in size and spherical in form. The crystalline nature of AgNPs was revealed by the XRD and SAED patterns. The catalytic capabilities of AgNPs were studied by reducing model pollutants such as MB and RhB in the presence of NaBH4 as a reducing agent. Kinetic investigations indicated that the reduction of these pollutants followed pseudo-first order kinetics, with rate constants of 0.296 min^{-1} for MB and 0.335 min^{-1} for RhB.

5. ACKNOWLEDGEMENTS

All the authors thankful to the department of chemistry, Osmania University for providing necessary facilities to conduct the experiments

Conflict of interest

The authors declare no conflicts of interest.

6. REFERENCES

1. MeenaKumari M, Philip D.*Spectrochim. Acta Part A Mol. Biomol. Spectrosc.*, 2015;**135**:632-638.
2. Bhagavanth reddy G, Dadigala R, Bandi R, Seku K, Koteswararao D, Girija Mangatayaru K, Esmail Shalan A.*RSC Adv.*, 2021; **11**:5139-5148.
3. Bandi R, Alle M, Park C.W, Han S.Y, Kwon G.K, Kim J.C, Lee S.H.*Carbohydr. Polym.*, 2020; **240**:116356.
4. Kaushik M, Moores A.*Green Chem.*, 2016; **18**:622-637.
5. Kumar V, Singh D.K, Mohan S, Bano D, Gundampati R.K, Hasan S.H.*J. Photochem. Photobiol. B Biol.*, 2017; **168**:67-77.
6. Ahmad S, Munir S, Zeb N, Ullah A, Khan B, Ali J, Bilal M, Omer M, Alamzeb M, Salman S.M, Ali S.*Int. J. Nanomedicine*, 2019; **14**:5087-5107.
7. Rafique M, Sadaf I, Rafique M.S, Tahir M.B.*Artif. Cells, Nanomedicine Biotechnol.*, 2017; **45**:1272-1291.
8. Ahmed S, Ahmad M, Swami B.L, Ikram S.*J. Adv. Res.*, 2016; **7**:17-28.
9. Vuolo MM, Lima GC, Maróstica MR. *Flour and Breads and Their Fortification in Health and Disease Prevention*, 2019; 249-258.
10. 1My-Thao Nguyen T, Anh-Thu Nguyen T, Tuong-Van Pham N, Ly QV, Thuy-Quynh Tran T, Thach TD et al. *Arab. J. Chem.*, 2021;**14**:103096.
11. Nthunya LN, Derese S, Gutierrez L, Verliefde AR, Mamba BB, Barnard TG,Mhlanga SD. *New J. Chem.*, 2019; **43**:4168-4180.
12. Ayinde WB, Gitari WM, Samie A.*Green Chem. Lett. Rev.*, 2019; **12**:225-234.
13. Amendola V, Bakr OM, Stellacci F.*Plasmonics*, 2010; **5**:85-97.
14. Handayani W, Ningrum AS, Imawan C. *Journal of Physics:Conference Series*, 2020; **1428**:12021.
15. Su Y, Shi B, Liao S, Zhao J, Chen L, Zhao S. *ACS Sustain. Chem. Eng.*, 2016; **4**:1728-1735.
16. Song J, Roh J, Lee I, Jang J. *Dalt. Trans.*, 2013;**42**:13897-13904.
17. Rostami-Vartooni A, Nasrollahzadeh M, Alizadeh M. *J. Colloid Interface Sci.*, 2016; **470**:268-275.
18. Gangapuram B.R, Bandi R, Alle M, Dadigala R, Kotu GM, Guttena V. *J. Mol. Struct.*, 2018;**1167**:305-315.
19. Kora AJ, Rastogi L. *Arab. J. Chem.*, 2018; **11**:1097-1106.
20. Garg N, Bera S, Rastogi L, Ballal A, Balaramakrishna MV. *Spectrochim. Acta Part A Mol. Biomol. Spectrosc.*, 2020; **232**:118126.